

# Naphthalene degradation in water by heterogeneous photocatalysis: An investigation of the influence of inorganic anions

Antoine Lair\*, Corinne Ferronato, Jean-Marc Chovelon,  
Jean-Marie Herrmann

IRCELYON, Institut de Recherche sur la Catalyse et l'Environnement de Lyon,  
UMR CNRS 5256, Université de Lyon, Villeurbanne F-69626, France

Received 27 March 2007; received in revised form 19 June 2007; accepted 19 June 2007  
Available online 23 June 2007

## Abstract

In a pollution control context, the degradation of naphthalene in water was performed by photocatalysis in UV-irradiated TiO<sub>2</sub> suspensions. The influence of physicochemical parameters such as concentration, photonic flux, temperature, pH and mass of catalyst has been investigated. An optimum titania concentration was found equal to 2.5 g L<sup>-1</sup>. This value is identical to that observed in other liquid phase reactions, either in water or in liquid organic phases, confirming that this value depends on the design of the photoreactor (geometry, texture of the catalyst, optical pathway). The almost nil effect of the pH upon the kinetics indicates that protons do not intervene at the limiting step level. It was also confirmed that the kinetics were slightly accelerated by a limited increase in temperature with a small apparent activation energy of reaction equal to 22 kJ mol<sup>-1</sup>. The presence of common salts generally found in natural waters was followed versus kinetics, including NaCl to simulate the treatment of seawater. It has been found that small amounts of carbonates strongly inhibit naphthalene adsorption and degradation. Hydrogenocarbonates were also found to inhibit naphthalene adsorption at low concentration, but no inhibition was observed at concentrations below 0.3 mol HCO<sub>3</sub><sup>-</sup> L<sup>-1</sup>. Surprisingly, addition of sodium chloride makes the initial reaction faster and more selective. It was interpreted as an enhancement of naphthalene adsorption by sodium chloride. The main intermediates of naphthalene photodegradation have been identified by HPLC–DAD and GC–MS. They result from naphthalene hydroxylation and ring-cleavage by action of oxygenated radicals.

© 2007 Elsevier B.V. All rights reserved.

**Keywords:** Naphthalene degradation; Photocatalysis; Photocatalytic degradation; TiO<sub>2</sub>; Titania

## 1. Introduction

Naphthalene is a common polycyclic aromatic hydrocarbon (PAH) which can be found in many anthropogenic fluxes, such as combustion fumes, used oil, bilge water, etc. Since it is the most water-soluble PAH (solubility 25–30 mg L<sup>-1</sup> at ambient temperature), it is the dominant one in water. It has been considered as possibly carcinogenic to humans (US EPA 1998, IARC 2002), and it has both acute and chronic effects on human and animal health.

Removing traces of naphthalene from water (directly contaminated or used for soil washing) is possible via many techniques, including biofiltration [1], bioreactors [2], membrane biore-

actors [3], ozonolysis [4,5], pulse radiolysis [6,7], electron beam irradiation [8], electrolytic aeration [9] and photocatalysis [10–18].

Photocatalysis is based on the activation of a semiconductor surface (most often TiO<sub>2</sub>), by UV radiation below 380 nm, which releases electrons from the semiconductor's valence band. Photogenerated electrons and holes react then with water, dissolved oxygen and organic compounds to form radicals, making a strongly oxidant environment [19]. Photocatalysis presents critical advantages over other techniques. It is faster than bioreactors and cheaper than ozonolysis and radiolysis. Furthermore it can be achieved under direct sunlight, making it cheaper to operate and independent from any power source.

The literature about naphthalene oxidation by photocatalysis shows that degradation yields various compounds such as naphthols, naphthoquinones and cinnamaldehydes, and that naphthalene is finally completely mineralized into CO<sub>2</sub> and

\* Corresponding author: IRCELYON, Université Lyon 1, Villeurbanne F-69626, France. Tel.: +33 472448405; fax: +33 472448438.

E-mail address: [antoine.lair@ircelyon.univ-lyon1.fr](mailto:antoine.lair@ircelyon.univ-lyon1.fr) (A. Lair).

H<sub>2</sub>O. However, there is a lack for kinetic data for naphthalene degradation in environmental conditions. Indeed, a lot of authors used cosolvents (acetonitrile, ethanol) that help dissolving naphthalene, but change the rate and the selectivity of the reaction [11,13,14,16]. Only two references investigate the effect of non-ionic surfactants and organic contaminants from soil [10,18].

In this paper, the degradation of naphthalene by photocatalysis was studied from the kinetic point of view, as well as the pathway that leads to the major products. The kinetic study allowed us to determine the effect of physical parameters such as temperature and photonic flux, and chemical parameters such as pH and the presence of inorganic ions such as hydrogenocarbonate, carbonate and chloride.

## 2. Experimental

### 2.1. Materials and reagents

Naphthalene, sodium carbonate, sodium hydrogenocarbonate and sodium chloride were purchased from Aldrich (St. Quentin-Fallavier, France) and were used as received. The following compounds were used for intermediates identification and were also purchased from Aldrich: 1-naphthol, 2-naphthol, naphthazarin, cinnamaldehyde, *o*-phthalaldehyde, 2-methylbenzofuran, 1,5-dihydroxynaphthalene, 1,7-dihydroxynaphthalene, 1,3-indandione, salicylaldehyde, 2,3-dihydroxybenzaldehyde, phthalic acid, phthalide, and coumarin.

Acetonitrile used as HPLC eluent and methanol used as SPE solvent were purchased from SDS Carlo Erba (Peypin, France).

Millipore deionized water was used for dilution and HPLC elution. The photocatalyst was TiO<sub>2</sub> Degussa P-25 (specific area 50 m<sup>2</sup> g<sup>-1</sup>, mean particle size of ca. 30 nm).

### 2.2. Photoreactor

The adsorption and irradiation experiments were carried out in a 60 mL jacketed glass flask with a Pyrex bottom of 30 mm in diameter [20]. The light source was a Philips HPK 125 W mercury lamp, emitting in the near-UV (mainly around 365 nm), with a Corning 0–52 filter to avoid direct photolysis of naphthalene by UV-irradiation below 340 nm. IR radiations were filtered out by water circulating in the reactor jacket. The flux of photons entering the reactor was directly determined, using uranyle oxalate as an actinometer. It could be reduced by placing metallic grids between the lamp and the reactor. For all experiments, the suspensions were magnetically stirred without any permanent air bubbling. In these conditions, the oxygen dissolved in water following Henry's law was sufficient to ensure a constant oxygen pressure and a constant resulting coverage of the surface of titania [19]. Table 1 gives the standard conditions used for the study.

### 2.3. Procedure

Temperature was fixed at 20 °C and controlled throughout the experiment. Unless required, pH was not initially modified

Table 1  
Standard conditions used for the kinetic study on naphthalene

Volume of titania suspension	25 mL
Temperature	$T = 20\text{ }^{\circ}\text{C}$
pH before irradiation	4.4
Naphthalene concentration	5 ppm/40 μM
Mass concentration of suspended TiO <sub>2</sub>	2.5 g L <sup>-1</sup>
Time for pre-adsorption in the dark	30 min
Main irradiation wavelength	$\lambda = 365\text{ nm}$
Efficient photonic flux	$\phi = 5.4 \times 10^{15}\text{ photons s}^{-1}$

or controlled in the reactor. When required, initial pH values were adjusted using NaOH or HNO<sub>3</sub>. We used a standard initial naphthalene concentration of 40 μmol L<sup>-1</sup> (5 ppm).

A volume of 25 mL of aqueous naphthalene solution was introduced in the reactor and vigorously stirred. Once thermal and volatilization equilibria reached, 62.5 mg of TiO<sub>2</sub> powder was introduced in the reactor. Solution was then stirred in the dark during 30 min to reach adsorption equilibrium.

During kinetic experiments, 300 μL aliquots were sampled before introduction of TiO<sub>2</sub>, during adsorption and at different irradiation times. Samples were filtered through 0.45 μm PTFE Millipore filters, and immediately analysed by HPLC. Analytical uncertainty on naphthalene concentration was mainly due to the filtration step and has been evaluated to be 1.5 μmol L<sup>-1</sup>.

### 2.4. Analyses

High performance liquid chromatography (HPLC) analyses were performed using a Shimadzu HPLC system with a diode array detector (DAD) and a Uptisphere C18 HDO column (stationary phase 3 μm, dimensions 150 mm × 3 mm). Mobile phase was a mixture of water and acetonitrile, with a ratio of 90% (v/v) acetonitrile at a flow rate of 0.5 mL min<sup>-1</sup>. A gradient elution was used to separate reaction intermediates: from 15% to 50% acetonitrile in 30 min, then from 50% to 100% acetonitrile in 10 min.

Gas chromatography–mass spectrometry (GC/MS) analyses of intermediate products were performed after solid phase extraction (SPE) of 25 mL irradiated solution on Isolute C18 cartridges and elution with 1 mL methanol. The concentration efficiency varied from 10% to 30% depending on the compound.

GC–MS analyses were performed on a Perkin Elmer Clarus 500 system, with a capillary Elite 5MS column (length: 60 m, internal diameter: 0.25 mm, film thickness: 1.0 μm). Injection was made at 250 °C with a split ratio of 5:1. The column temperature was held at 100 °C during 5 min, then raised at 10 °C min<sup>-1</sup> to 240 °C, and finally held at 240 °C during 30 min. Electron Ionization mass spectra were identified using NIST 2002 Library and most of these compounds were automatically identified by the NIST MS-Search software.

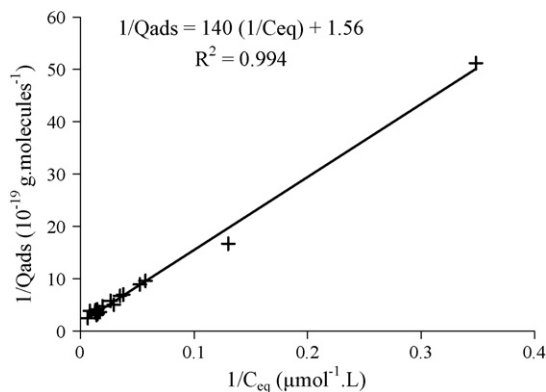


Fig. 1. Transformation of Langmuir isotherm:  $Q_{\text{ads}}^{-1} = f(C_{\text{eq}}^{-1})$ .

### 3. Results and discussion

#### 3.1. Adsorption of naphthalene in the dark

According to the Langmuir model, the coverage  $\theta$  at equilibrium varies as

$$\theta = \frac{Q_{\text{ads}}}{Q_{\text{max}}} = \frac{K_L C_{\text{eq}}}{1 + K_L C_{\text{eq}}} \quad (1)$$

where  $Q_{\text{ads}}$  is the number of adsorbed naphthalene molecules,  $Q_{\text{max}}$  the maximum number of molecules that can be adsorbed on the surface,  $C_{\text{eq}}$  the concentration at adsorption equilibrium and  $K_L$  the Langmuir adsorption constant.

The linear plot in Fig. 1 can be identified with:

$$\frac{1}{Q_{\text{ads}}} = \frac{1}{Q_{\text{max}}} + \frac{1}{(Q_{\text{max}} K_L C_{\text{eq}})} \quad (2)$$

The intercept at the origin gives  $Q_{\text{max}}$  and the slope gives  $K_L$  via the product  $K_L Q_{\text{max}}$ . Table 2 gives the adsorption constants measured. We found a value of  $4100 \text{ L mol}^{-1}$  for  $K_L$  and  $24 \mu\text{mol g}^{-1}$  for  $Q_{\text{max}}$ . Coverage ranges from 0.06 to 0.38 when naphthalene concentration ranges from  $15.9$  to  $175 \mu\text{mol L}^{-1}$ . At concentrations below  $40 \mu\text{mol L}^{-1}$ , adsorption equilibrium can be approximated by a linear law, where  $Q_{\text{ads}} = K_L \times Q_{\text{max}} \times C_{\text{eq}}$ .

Another value of the adsorption constant  $K_L$  was given by Barrios et al. [18] ( $K_L = 1152 \text{ L mol}^{-1}$ ) in phosphate buffer and Triton X-100 surfactant. This value is lower because of the competitive adsorption of phosphate ions and surfactant molecules.

#### 3.2. Effect of naphthalene concentration

Fig. 2 shows the two steps of preliminary adsorption and photodegradation. In standard conditions given in Table 1, naph-

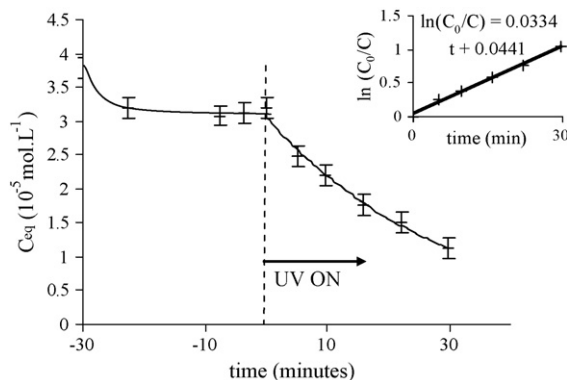


Fig. 2. Evolution of naphthalene concentration in standard conditions of dark adsorption and photocatalytic disappearance. The inset shows the logarithmic representation of naphthalene conversion vs. irradiation time.

thalene half-life time is less than 30 min. Photodegradation was carried on different initial naphthalene concentrations, with a constant photon flux. When plotting the initial reaction rate versus the initial equilibrium concentration (Fig. 3), it can be observed that reaction rate increases linearly with concentration, up to  $40 \mu\text{mol L}^{-1}$ . At higher concentrations, there is a clear deviation from linearity and the reaction rate increases more slowly with increasing initial concentration. Since solubility of naphthalene is very low ( $200\text{--}250 \mu\text{mol L}^{-1}$ ), it was not possible to investigate higher concentrations to clearly identify a saturation behaviour. However, this saturation seems to occur at much lower concentration than the adsorption saturation.

We tried to verify if this behaviour was consistent with the Langmuir–Hinshelwood (LH) mechanism, which is, for practical and historical reasons, the most widely used to describe heterogeneous photocatalysis reactions [19,21]. According to the LH model, the reaction rate  $r$  varies proportionally with the coverage  $\theta$  as:

$$r = k_{\text{LH}}\theta = k_{\text{LH}} \left( \frac{K_L C_{\text{eq}}}{1 + K_L C_{\text{eq}}} \right) \quad (3)$$

where  $C_{\text{eq}}$  is the concentration at adsorption equilibrium,  $K_L$  is the Langmuir adsorption constant and  $k_{\text{LH}}$  is the apparent LH rate constant for the reaction. Then, if we plot  $1/r$  versus  $1/C_{\text{eq}}$ ,

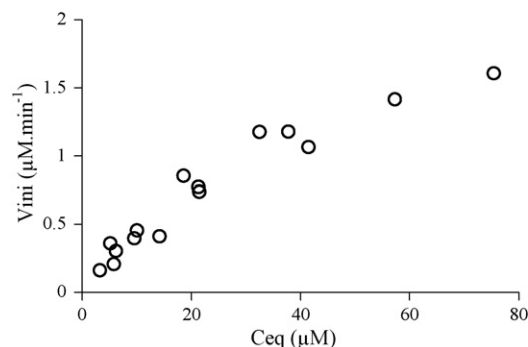


Fig. 3. Plot of the initial disappearance rate vs. initial naphthalene concentration.

Table 2

Adsorption constants of naphthalene on  $\text{TiO}_2$  P-25

$K_L$ ( $\text{L mol}^{-1}$ )	$4100 \pm 100$
$Q_{\text{max}}$ ( $\mu\text{mol g}^{-1}$ )	$24 \pm 3$
$Q_{\text{max}}$ ( $\text{molecules nm}^{-2}$ )	0.29

the equation becomes:

$$\frac{1}{r} = \frac{1}{K_L k_{LH}} \frac{1}{C_{eq}} + \frac{1}{k_{LH}} \quad (4)$$

With a photon flux of  $3.6 \times 10^{16}$  photons  $s^{-1}$ , the linearization of the LH equation gives  $k_{LH} = 2.2 \mu\text{mol min}^{-1}$  and  $K_L \times k_{LH} = 0.054 \text{ min}$ . It gives an alternate value of the adsorption constant:  $K_L = 25,000 \text{ L mol}^{-1}$ , which is inconsistent with the value of Langmuir adsorption constant found in the absence of reaction ( $K_L = 4100 \text{ L mol}^{-1}$ ). This confirms that the rate plateau occurs far before adsorption saturation. Values of  $K_L$  obtained at three different photon fluxes show that  $K_L$  decreases with light intensity, meaning that a phenomenon of naphthalene photodesorption might occur.

This deviation from the ideal Langmuir–Hinshelwood behaviour has been observed with many organic compounds and well discussed by Emeline et al. [21]. In short, the reactant concentration is less rate-determining when working with high photon fluxes, since adsorption equilibrium cannot be reached and photodesorption can happen. More generally, we are aware that the introduction of the parameter “light” in the heterogeneous photocatalytic system makes it differ from a well understood heterogeneous catalytic system.

However the first order approximation is still correct at low concentrations. For this reason, and because naphthalene is not likely to be found at concentrations above  $60 \mu\text{mol L}^{-1}$  in natural or artificial effluents, we chose to work with concentrations below  $40 \mu\text{mol L}^{-1}$  for the rest of this study. In these conditions, reaction is of first order with respect to naphthalene concentration and the disappearance rate can be expressed as:

$$r = \frac{-dC}{dt} = k_1 C_{eq} \quad (5)$$

We determined the first order rate constant  $k_1$  by measuring the slope of the  $\ln(C_{eq}/C(t)) = f(t)$  plot at the beginning of the reaction, at low conversions (below 20%).

### 3.3. Effect of catalyst loading

We measured the first order rate constant at different catalyst loadings, as shown on Fig. 4. It increases first linearly when increasing the catalyst loading to reach a maximum at about

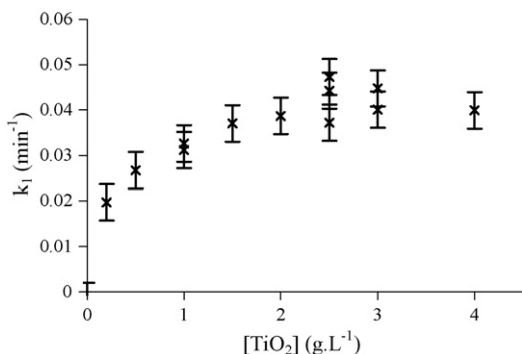


Fig. 4. Effect of catalyst mass (TiO<sub>2</sub> P-25).

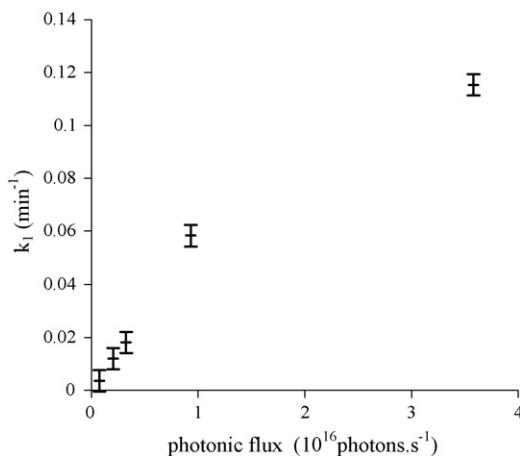


Fig. 5. Effect of photonic flux on the degradation rate.

$2.5 \text{ g L}^{-1}$ . Since this optimum value is identical to that observed in other liquid phase reactions, either in water or in liquid organic phases [20], it seems to depend only on the design of the photoreactor (geometry, texture of the catalyst, optical pathway). The existence of a threshold is attributed to a screening effect of TiO<sub>2</sub> particles as their concentration increases. The supplementary number of adsorption sites cannot then compensate the loss of photon flux by reflexion and diffusion.

### 3.4. Effect of the photonic flux

We observed different degradation rates when working with different photonic fluxes. Up to an incident photonic flux of  $10^{16}$  photons  $s^{-1}$  received by the suspension, the first order rate constant increases almost linearly, as shown in Fig. 5. This is consistent with a linear increase in the photogeneration of active species via the dissociation of electron–holes pairs at the surface of the photocatalyst. Beyond this range, the increase in the photonic flux does not induce a proportional increase in the degradation rate. The additional photons equally increase the concentration in electrons and holes, which favour their recombination rate. Emeline et al. [21] described this phenomenon as a first order law which tends to an order between 0 and 1 when recombination becomes abundant. Economically speaking, there is no interest in increasing the photon flux any more since part of it contributes to a sterile electron–hole recombination, i.e. to a qualitative degradation of UV-light energy.

In the photonic flux range below  $10^{16}$  photons  $s^{-1}$  and at a naphthalene concentration of  $40 \mu\text{mol L}^{-1}$ , a value of quantum yield has been calculated to be  $5 \times 10^{-2} \text{ mol E}^{-1}$ .

### 3.5. Effect of temperature

As can be seen in Fig. 6, the reaction rates reasonably follow the Arrhenius law in the temperature range studied (10–40 °C):

$$k_1 = k_0 \exp\left(\frac{-E_a}{RT}\right) \quad (6)$$

As expected [22], the value of the activation energy  $E_a$  is quite low:  $E_a = 22 \pm 2 \text{ kJ mol}^{-1}$ . Since the photoactivation pro-

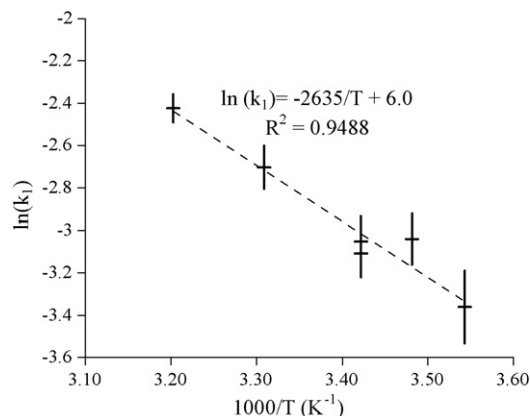


Fig. 6. Arrhenius plot of naphthalene degradation ( $T$  from 10 °C to 40 °C).

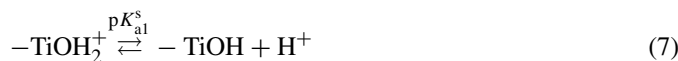
cess is irrelevant to thermal activation, the activation energy found is only apparent. Its (slightly) positive value indicates that temperature concerns the desorption of first step intermediates in the medium [19]. This measured value might be exaggerated because of the effect of naphthalene volatilization, which accelerates when temperature increases.

### 3.6. Effect of pH

A fast pH fall, of about 2 units, is observed when  $\text{TiO}_2$  is added in the solution. This fall is attributed to the hydration of the surface of  $\text{TiO}_2$ . Water is dissociated into hydroxide ions that are strongly adsorbed at the surface and into protons that are released in the liquid phase. This pH fall was noticed in the absence of mineral ions, whatever the initial pH value (pH 3–11). In pure water, pH falls from 6.0 to 4.4 when  $\text{TiO}_2$  is added, whereas the fall is negligible when carbonates or hydrogenocarbonates are present, since the solution is buffered. Increasing ionic strength by addition of NaCl also attenuates the pH drop.

Another slight decrease in pH is noticed when the solution is irradiated. This can be attributed to the production of transient acidic products resulting from naphthalene degradation. Let us recall that carboxylic acids are the successive sources of  $\text{CO}_2$  evolution by following the “photo-Kolbe” reaction as mentioned in Ref. [19].

It is important to know the effect of pH on surface charges of  $\text{TiO}_2$ . When  $\text{TiO}_2$  surface is hydrated, the principal surface functionality is the amphoteric “titanol” moiety,  $-\text{TiOH}$ , which takes part in the following acid-base equilibrium:



where  $pK_{a1}^s$  and  $pK_{a2}^s$  represent the negative log of the acidity constants of the first and second acid dissociation, respectively. The pH of zero point of charge,  $\text{pH}_{\text{zpc}}$ , is given by the following equation:

$$\text{pH}_{\text{zpc}} = \frac{1}{2}(pK_{a1}^s + pK_{a2}^s) \quad (9)$$

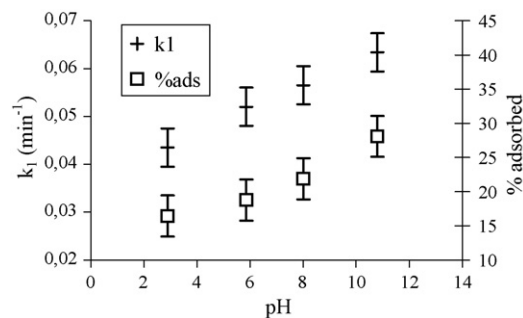


Fig. 7. Effect of pH on adsorption and degradation kinetics.

For titania Degussa P-25, the corresponding surface acidity constants are found to be:  $pK_{a1}^s = 4.5$  and  $pK_{a2}^s = 8$ , and  $\text{pH}_{\text{zpc}}$  has been determined by titration:  $\text{pH}_{\text{zpc}} = 6.3$  [23].

Fig. 7 presents the variation of the first order rate constant and the quantity of adsorbed naphthalene as a function of pH. We notice a higher adsorption at higher pH, which is assumed to be linked to double layer modification at the surface. A maximum of adsorption was expected around  $\text{pH}_{\text{zpc}}$ , since naphthalene is a hydrophobic neutral compound. This was not observed in this case, because the solutions at different pH had different ionic strength:  $\text{HNO}_3$  was present at pH 3 and  $\text{NaOH}$  was present at pH 8 and 11, whereas no ionic species were added at natural pH 6. After additional adsorption experiments at similar ionic strengths (addition  $0.6 \text{ mol/L}^{-1}$  NaCl), we can show that adsorption is significantly higher at pH 5.8 than at pH 2.5 and 10.8.

The linear increase in the degradation rate is due to the better adsorption of naphthalene, but it can also be explained by the increase in  $\text{OH}^\bullet$  radicals production due to a higher concentration of  $\text{OH}^-$  ions in the solution [24].



The kinetic order with respect to proton concentration was calculated by plotting  $\log(k_1)$  against pH. It was found that  $k_1$  varies proportionally to  $[\text{H}^+]^{-0.02}$ . According to chemical kinetics, this means that protons do not intervene in the rate-limiting step of the reaction. The negative sign is indicative of a limited inhibiting effect.

### 3.7. Effect of inorganic ions

To investigate the effect of some inorganic salts that are most likely to be found in natural waters, sodium carbonate, sodium hydrogenocarbonate and sodium chloride were added at different concentrations in the initial solution and the corresponding first order rate constants were measured. Similarly, the influence of those inorganic ions on naphthalene adsorption was also followed. Results can be interpreted by considering adsorption, radical reactions and double layer theory.

#### 3.7.1. Carbonate ions

Fig. 8 shows that carbonates inhibit both naphthalene adsorption on  $\text{TiO}_2$  and the disappearance rate constant. At alkaline pH, carbonate anions are supposed to be repelled by the negatively

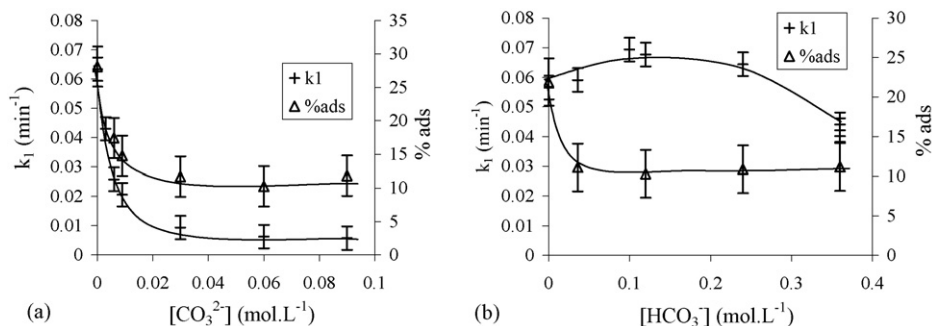
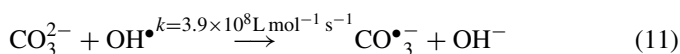


Fig. 8. Effect of  $[\text{CO}_3^{2-}]$  and  $[\text{HCO}_3^-]$  on kinetics and adsorption. (a)  $[\text{CO}_3^{2-}]$  between 0 and 0.09  $\text{mol.L}^{-1}$  (initial without  $\text{TiO}_2$  pH  $\approx 11$ ). (b)  $[\text{HCO}_3^-]$  between 0 and 0.36  $\text{mol.L}^{-1}$  (initial pH without  $\text{TiO}_2$   $\approx 8.5$ ).

charged  $\text{TiO}_2$  surface. However, according to the double layer model, they accumulate near the surface in the Gouy–Chapman layer, which superimposes the Stern dense layer where sodium cations are strongly attracted by the negative  $\text{TiO}_2$  surface.

Radical scavenging can explain why degradation is even more inhibited by carbonates than adsorption. Carbonate ions are known to strongly scavenge hydroxyl radicals [25]:

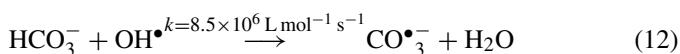


For comparison, the first order rate constant of the reaction of naphthalene with  $\text{OH}^\bullet$  is estimated to be  $1.2 \times 10^{10} \text{ L mol}^{-1} \text{ s}^{-1}$  [25]. The carbonate radicals that are formed can theoretically react with naphthalene. However, they have a lower oxidation potential than hydroxyl radicals ( $E_0(\text{CO}_3^{\bullet-}/\text{CO}_3^{2-}) = 1.85 \text{ V}$ ,  $E_0(\text{OH}^\bullet/\text{H}_2\text{O}) = 2.80 \text{ V}$ ), so that their reaction on naphthalene is less easy to initiate.

### 3.7.2. Hydrogenocarbonate ions

The influence of hydrogenocarbonate ions concentration on degradation rate is shown in Fig. 8. In natural waters (pH 6.5–8.5), hydrogenocarbonate ions are more present than the carbonate ones ( $\text{p}K_a \text{ HCO}_3^-/\text{CO}_3^{2-} = 10.2$ ), and their concentration rarely exceeds 0.05  $\text{mol.L}^{-1}$ . At this concentration, there is no noticeable effect of hydrogenocarbonates on degradation. We notice a slight acceleration of the reaction while adding  $\text{HCO}_3^-$  up to 0.1  $\text{mol.L}^{-1}$ . This acceleration might originate from the increase in pH (from pH 6 to 8). We extended the hydrogenocarbonates concentration range to investigate effects at higher concentration. Once adding more hydrogenocarbon-

ates, which has no further effect on pH, an inhibition of naphthalene degradation begins to be observed. As for carbonates, this effect has been formerly attributed to adsorption competition, which seems anyway to reach a plateau at  $\text{HCO}_3^-$  concentrations above 0.1  $\text{mol.L}^{-1}$ , and scavenging of hydroxyl radicals. Indeed hydrogenocarbonates react with hydroxyl radicals [25]:



Compared with carbonates, hydrogenocarbonates scavenge 50 times less hydroxyl radicals. Hence they are less inhibiting the reaction and other parameters, such as pH, can moderate inhibition at low concentrations.

### 3.7.3. Chloride anions

Fig. 9 presents the variation of  $k_1$  with respect to the concentration of chloride ions, added as sodium chloride in the initial solution. The result is a clear increase in both adsorbed quantity and reaction rate, which was unexpected. Indeed, in the case study of many compounds, chloride was found to inhibit both adsorption and photodegradation at  $\text{pH} < \text{pH}_{\text{pzc}}$ , when  $\text{TiO}_2$  surface is positively charged [26,27]. In our experiments, final pH was 5.7, i.e. slightly below the  $\text{pH}_{\text{pzc}}$  of  $\text{TiO}_2$ , and addition of sodium chloride was expected to decrease the reaction rate.

A first possible hypothesis was a strong increase in naphthalene volatilization due to an increased ionic strength, but isolated experiments showed that volatilization was still negligible with respect to degradation. A second possible explanation was that chloride anions, as other halides, are known to scavenge

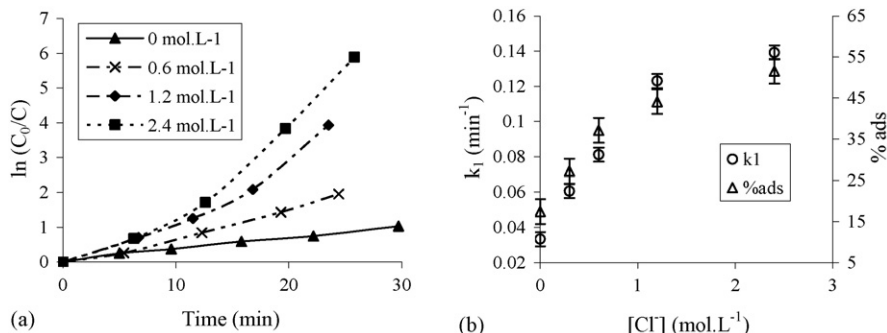


Fig. 9. (a) Time evolution of naphthalene concentration at different concentrations of  $\text{Cl}^-$ . (b) Effect of  $[\text{Cl}^-]$  on first order kinetic constant.

photogenerated holes [28]. They are oxidized by photoholes to chlorine radicals which are reduced back by electrons to chloride ions, hence reducing the availability of holes and electrons. Chlorine radicals can react with organic compounds via addition/elimination reactions ( $E_0(\text{Cl}^\bullet/\text{Cl}^-) = 2.5 \text{ V}$ ) [29]. However, GC–MS analyses did not detect any chlorinated compounds after irradiation, showing that reactions of addition with chlorine radicals are negligible in these conditions.

We found an increased adsorption with increasing salt concentration. Such a “salting out” phenomenon has been observed by other authors [30,31]: an increase in ionic strength causes a decrease in the solubility of neutral organics such as naphthalene and favours hydrophobic adsorption. For example, Karickhoff et al. [31] found that pyrene sorption increased by 15% with an increase of salinity from 0 to 0.34 M sodium chloride. According to the Setschenow law and constants provided by the IUPAC NIST Solubility Database, the solubility of naphthalene decreases quite linearly from 31.7 to 9.8 mg L<sup>-1</sup> (respectively 248–76 μmol L<sup>-1</sup>), when chloride concentration varies between 0 and 2.4 mol L<sup>-1</sup>. A decrease in solubility causes the precipitation of naphthalene on the surface of TiO<sub>2</sub>. The increase of reactant concentration on the surface might be the only explanation for the reaction rate enhancement. It is important to note that this phenomenon is inconsistent with the hypothesis of monolayer adsorption of the Langmuir–Hinshelwood model. Comparative adsorption experiments showed a similar adsorption enhancement of NaCl and KCl (concentration 0.6 mol L<sup>-1</sup>), but no increase in adsorption was noticed with NaBr.

The effect of NaCl addition on naphthalene degradation has to be taken carefully when comparing naphthalene with the primary products that are formed. Fig. 10 compares the evolution of naphthalene concentration with those of the two most abundant primary reaction intermediates, with and without NaCl. It can be seen that when sodium chloride is added, naphthalene disappears faster, as already noticed, but the two main primary products tend to accumulate more in the solution than in absence of sodium chloride. These products are more hydrophilic than naphthalene, and their adsorption is inhibited by sodium chloride, as noticed for many other compounds. Hence they are more slowly transformed into secondary products. In conclusion, addition of NaCl is not expected to have an accelerating effect on the whole mineralization process.

We performed the degradation of naphthalene in a mixture of sodium chloride (0.6 mol L<sup>-1</sup>) and sodium hydrogenocarbonate (0.03 mol L<sup>-1</sup>) to determine the rate of degradation in near-

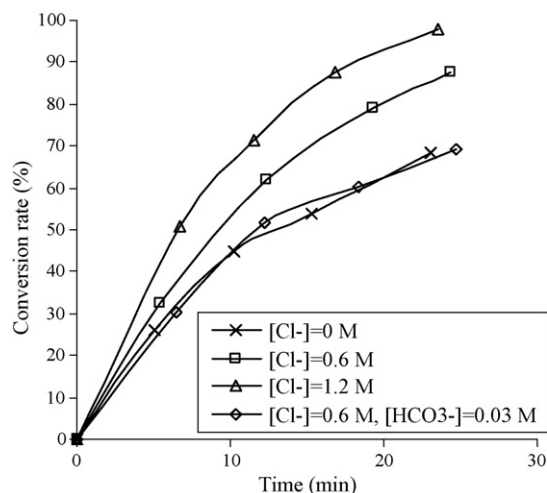


Fig. 11. Evolution of conversion rate for different chloride concentrations.

seawater conditions (hydrogenocarbonate ions make pH raise to 8.4). In Fig. 11, we can see that sodium chloride has no noticeable effect on the reaction kinetics when sodium hydrogenocarbonate is present.

### 3.8. Reaction intermediates and pathway

#### 3.8.1. GC–MS analyses

GC–MS analyses revealed a series of peaks at different retention times, from 15 to 24 min, naphthalene being the less retained compound.

A dozen of peaks were identified (Table 3). The most abundant one is by far the peak of compound IX, with  $t_R = 21 \text{ min}$ . The mass spectrum of this compound was found by other authors and identified as 2-formylcinnamaldehyde (IX). It was also identified by NMR and FTIR [14,13,16,32]. Pramauro et al. [10] identified this spectrum as benzalmalonic dialdehyde, but no simple mechanism can explain the formation of such a compound. 2-Formylcinnamaldehyde is also a major product of naphthalene photolysis.

Other abundant peaks revealed the presence of naphthols, mainly 1-naphthol (V). Two other products, 1,4-naphthoquinone (III) and 1,2-benzenedicarboxaldehyde (II), were also found. The structures of three compounds remain unclear, each of them representing more than 1% of the total TIC area. They are shown in Table 4.

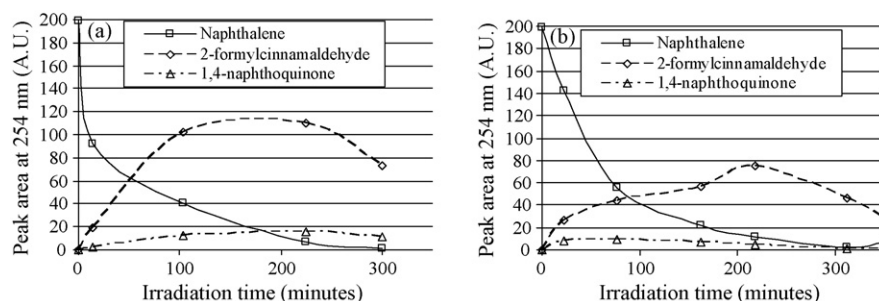
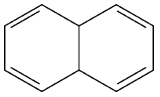
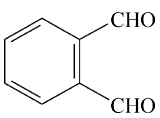
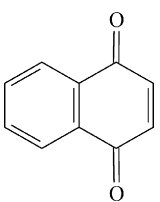
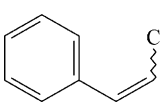
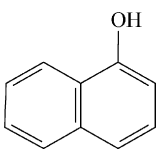
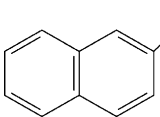
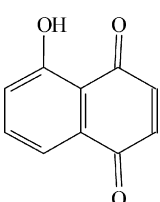
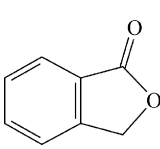
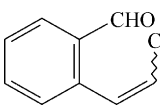
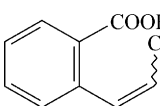
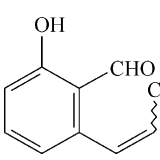


Fig. 10. Comparison of primary products evolution with 0.6 mol L<sup>-1</sup> NaCl (a) and pure water solution (b).

Table 3  
Main reaction intermediates, identified by GC–MS

No.	Structure	Name	Retention time (min)	Rel. TIC area (%) (120 min irradiation)	Present in Ref.
I		Naphthalene <sup>a</sup>	15.7	15	(Reactant)
II		1,2-Benzenedicarboxaldehyde <sup>a</sup>	16.6	3.5	[10,15,32]
III		1,4-Naphthoquinone <sup>a</sup>	19.4	2.0	[10,13–15,33]
IV		Cinnamaldehyde <sup>a</sup>	20.3	1.5	[13]
V		1-Naphthol <sup>a</sup>	20.7	8.7	[10,13–15,32,33]
VI		2-Naphthol <sup>a</sup>	20.8	1.0	[13–15]
VII		5-Hydroxy-1,4-naphthoquinone	20.9	0.3	
VIII		Phthalide <sup>a</sup>	21.0	0.1	[10]
IX		2-Formylcinnamaldehyde <sup>a</sup>	21.1	50	[13,14,16,32]
X		2-Carboxycinnamaldehyde	22.7	0.7	
XI		3-Hydroxy-2-formylcinnamaldehyde	23.2	3.7	[13]

<sup>a</sup> Identified by HPLC–DAD.



Table 4  
Main compounds not clearly identified by GC–MS

Retention time (min)	Relative TIC area (%)	Base peak ( $m/z$ )	Mass peak ( $m/z$ )	Probable structure/formula
19.0	3	133	164	
19.7	4	148	178	
21.4	3	116	162	$C_{10}H_{10}O_2$

5,8-Dihydroxynaphthoquinone (molecular mass 190) was detected as an intermediate by some authors who used FTIR and NMR [12,17], but no fragment with a  $m/z$  higher than 178 was presently found by GC–MS. Dihydroxynaphthalenes were not found in this study, although they were detected by other authors [10,11]. They might be formed during the reaction but might adsorb strongly on  $TiO_2$  as alcoholates, and not desorb into the solution.

### 3.8.2. HPLC analyses

HPLC–DAD allowed us to separate ca. 15 major products, with retention times ranging from 10 to 45 min. Most

of these products had retention times much lower than naphthalene, because of higher polarity. Twenty-three commercial products (cf §3.1 materials and reagents) chosen from assumptions and literature data were analysed and compared to the intermediates found in the UV-irradiated suspension. Seven compounds were clearly identified from both their retention time and their UV-spectrum. All of them were identified by GC–MS. The two most abundant products, having very close retention times, did not match any commercial compound. They were isolated using a fraction collector and analysed by GC–MS. Only one peak appeared, corresponding to 2-formylcinnamaldehyde. These two products were assumed to

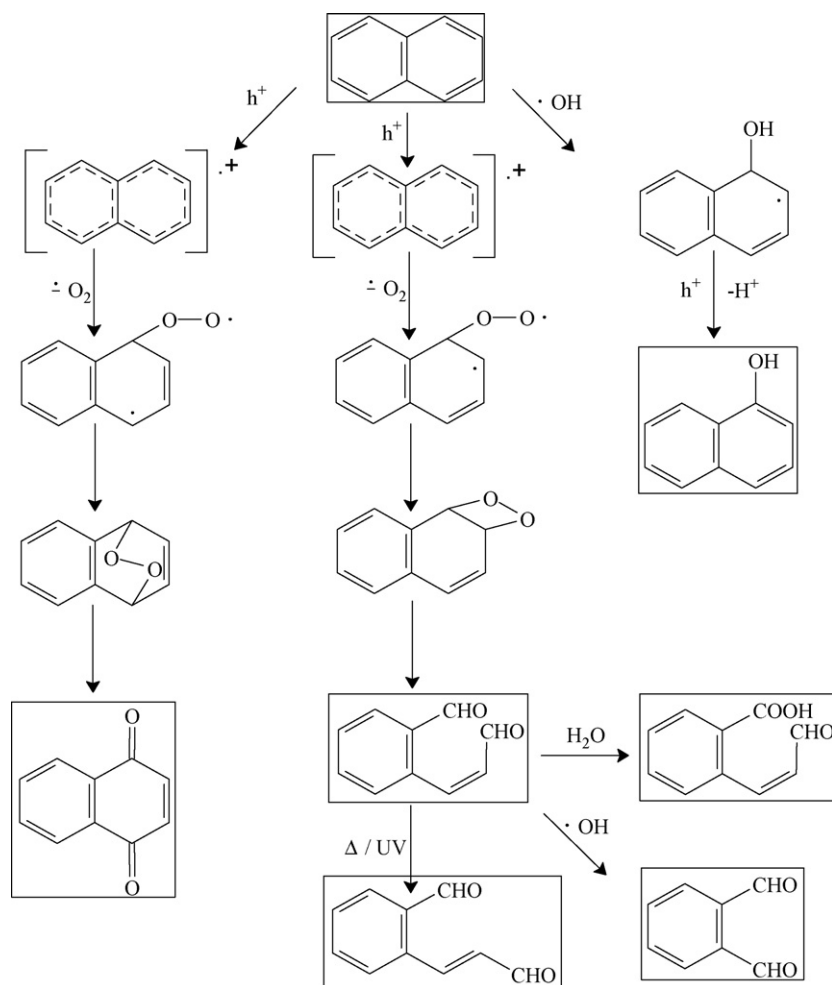


Fig. 12. Possible pathways for the formation of main intermediates of the naphthalene degradation.

be stereoisomers, one being *Z*-2-formylcinnamaldehyde and the other one being *E*-2-formylcinnamaldehyde. Ohno et al. [16] suggested that the *Z*-isomer was formed directly from naphthalene, and the *E*-isomer, thermodynamically more stable, was spontaneously formed from the *Z*-isomer. Both isomers could be separately identified by some authors who used NMR identification [12,16].

### 3.8.3. Reaction pathway

The formation of detected intermediates can be explained by the action of  $\text{OH}^\bullet$ ,  $\text{O}_2^{\bullet-}$  and/or  $\text{h}^+$  (Fig. 12). The opening of an aromatic cycle is the major route of transformation.

There is still some uncertainty about which of these radicals reacts to form quinones such as 1,4-naphthoquinone. The first hypothesis is a successive addition of two hydroxyl radicals on a cycle, leading to a naphthohydroquinone, which is next oxidized to the corresponding naphthoquinone [10,13,15]. The second possibility is an attack of naphthalene by a superoxide radical, leading to the formation of an unstable endoperoxide, which dissociates into a quinone [33]. However, since superoxide radical has a less reactivity, direct attack by superoxide is possible but rare. The last possibility is a direct oxidation of adsorbed naphthalene molecule by photogenerated holes to form naphthalene cation radical, and then the cation radical reacts with superoxide radical to form peroxide species which, in turn, dissociate into 1,4-naphthoquinone and/or 2-formylcinnamaldehyde.

Soana et al. [13] noticed that irradiation in pure acetonitrile gives mainly phthalic anhydride and 1,4-naphthoquinone, and the degradation rate was almost 10 times slower than in pure water. This shows that hydroxyl radical (produced from water) is the key species in naphthalene degradation, and that it must have no specific role in phthalic anhydride and 1,4-naphthoquinone formation.

Jia et al. [11] used a mixture of acetonitrile and water (94:6 in volume) as a solvent and saturated it with  $\text{O}_2$ . Only dihydroxynaphthalenes were formed.

The opening of the two cycles leads to the formation of smaller linear organic acids which are assumed to be gradually decarboxylated via a photo-Kolbe process [19]. This final process yields  $\text{CO}_2$  as the final product, which is evolved from the solution.

Total mineralization to carbon dioxide could not be presently investigated. However, Das et al. [12] and Pramauro et al. [10] measured the formation of carbon dioxide from the beginning of irradiation, showing that decarboxylation starts as soon as the first ring is opened. For example, the decarboxylation of 2-carboxycinnamaldehyde gives carbon dioxide and cinnamaldehyde (IV).

Half-time of  $\text{CO}_2$  formation was generally found to be thrice higher than that of naphthalene disappearance [10,12].

## 4. Conclusions

The photocatalytic degradation of naphthalene in aqueous solution was studied using  $\text{TiO}_2$  Degussa P-25 as a semiconductor catalyst. Adsorption of naphthalene plays an important role

in its degradation. The presence of carbonates and hydrogenocarbonates was found to inhibit adsorption and degradation of naphthalene, whereas sodium chloride at  $\text{pH} < \text{pH}_{\text{pzc}}$  accelerates the reaction through adsorption enhancement. More generally, this study points out the special behaviour of neutral PAH in wastewaters containing inorganic salts.

Naphthalene reacts with hydroxyl and superoxide radicals to yield naphthols, benzenic aldehydes and naphthoquinones. Naphthoquinones are naphthalene metabolites which are considered to be responsible for the toxicity of naphthalene [34]. For water treatment, the reaction time should be sufficient to let naphthoquinones be oxidized to less toxic compounds.

## Acknowledgement

This work was supported by a Délégation Générale de l'Armement (DGA) research grant.

## References

- [1] K. Maillacheruvu, S. Safaai, J. Environ. Sci. Health Part A: Toxic/Hazard. Subst. Environ. Eng. 37 (2002) 845–861.
- [2] J.R. Mihelcic, R.G. Luthy, Appl. Environ. Microbiol. 54 (1988) 1188–1198.
- [3] J.C. Ireland, D. Davila, H. Moreno, S.K. Fink, S. Tassos, Chemosphere 30 (1995) 965–984.
- [4] B. Legube, S. Guyon, H. Sugimitsu, M. Dore, Water Res. 20 (1986) 197–208.
- [5] K.A. Marley, R.A. Larson, P.L. Stapleton, W.J. Garrison, C.M. Klodnycky, Ozone: Sci. Eng. 9 (1987) 23–36.
- [6] N. Zevos, K. Sehested, J. Phys. Chem. 82 (1978) 138–141.
- [7] M. Roder, L. Wojnarovits, G. Foldiak, Radiat. Phys. Chem. 36 (1990) 175–176.
- [8] W.J. Cooper, M.G. Nickelsen, R.V. Green, S.P. Mezyk, Radiat. Phys. Chem. 65 (2002) 571–577.
- [9] R.K. Goel, J.R.V. Flora, J. Ferry, Water Res. 37 (2003) 891–901.
- [10] E. Pramauro, A.B. Prevot, M. Vincenti, R. Gamberini, Chemosphere 36 (1998) 1523–1542.
- [11] J. Jia, T. Ohno, Y. Masaki, M. Matsumura, Chem. Lett. 28 (1999) 963.
- [12] S. Das, M. Muneer, K.R. Gopidas, J. Photochem. Photobiol. A: Chem. 77 (1994) 83–88.
- [13] F. Soana, M. Sturini, L. Cermenati, A. Albini, J. Chem. Soc., Perkin Trans. 2 4 (2000) 699–704.
- [14] L. Hykrdova, J. Jirkovsky, G. Mailhot, M. Bolte, J. Photochem. Photobiol., A 151 (2002) 181–193.
- [15] J. Theurich, D.W. Bahnemann, R. Vogel, F.E. Ehamed, G. Alhakimi, I. Rajab, Res. Chem. Intermed. 23 (1997) 247–274.
- [16] T. Ohno, K. Tokieda, S. Higashida, M. Matsumura, Appl. Catal., A 244 (2003) 383–391.
- [17] B. Pal, M. Sharon, J. Mol. Catal. A: Chem. 160 (2000) 453–460.
- [18] N. Barrios, P. Sivov, D. D'andrea, O. Núñez, Int. J. Chem. Kinet. 37 (2005) 414–419.
- [19] J.-M. Herrmann, Top. Catal. 34 (2005) 49–65.
- [20] I. Bouzaida, C. Ferronato, J.M. Chovelon, M.E. Rammah, J.M. Herrmann, J. Photochem. Photobiol. A 168 (2004) 23–30.
- [21] A.V. Emeline, V.K. Ryabchuk, N. Serpone, J. Phys. Chem. B 109 (2005) 18515–18521.
- [22] J.-M. Herrmann, Catal. Today 53 (1999) 115–129.
- [23] N. Jaffrezic-Renault, P. Pichat, A. Foissy, R. Mercier, J. Phys. Chem. 90 (1986) 2733–2738.
- [24] J.-M. Herrmann, C. Guillard, P. Pichat, Catal. Today 17 (1993) 7–20.
- [25] G.V. Buxton, C.L. Greenstock, W.P. Helman, A.B. Ross, J. Phys. Chem. Ref. Data 17 (1988) 513–886.

- [26] A. Piscopo, D. Robert, J.V. Weber, *Catal. Appl. B* 35 (2001) 117–124.
- [27] H.Y. Chen, O. Zahraa, M. Bouchy, *J. Photochem. Photobiol. A* 108 (1997) 37–44.
- [28] P. Calza, E. Pelizzetti, *Pure Appl. Chem.* 73 (2001) 1839–1848.
- [29] P. Wardman, *J. Phys. Chem. Ref. Data* 18 (1989) 1637–1655.
- [30] R.P. Eganhouse, J.A. Calder, *Geochim. Cosmochim. Acta* 40 (1976) 555–561.
- [31] S.W. Karickhoff, D.S. Brown, T.A. Scott, *Water Res.* 13 (1979) 241–248.
- [32] M. Muneer, M. Qamar, D. Bahnemann, *J. Mol. Catal. A: Chem.* 234 (2005) 151–157.
- [33] M.J. Garcia-Martinez, L. Canoira, G. Blazquez, I. Da Riva, R. Alcantara, J.F. Llamas, *Chem. Eng. J.* 110 (2005) 123–128.
- [34] A. Pichard, Naphtalène—Fiche de données toxicologiques et environnementales des substances chimiques, INERIS (2004) 11.